2.N

Nuclear Physics **A231** (1974) 45—63; © *North-Holland Publishing Co., Amsterdam*

FUSION OF HEAVY NUCLEI IN A CLASSICAL MODEL

R. BASS

Institut für Kernphysik der Universität Frankfurt am Main, Germany

Received 16 April 1974

Abstract: The fusion of heavy nuclei is analyzed in a classical potential model. A quasi-elastic two-body potential is derived from the liquid drop model with inclusion of a finite range of interaction. Energy and angular momentum dissipation by friction are considered in the limit of strong localisation at the point of contact. The model suggests a classification of fragment pairs in terms of the parameter $x = (e^2/r_0 a_s)Z_1Z_2/A_1^{\frac{1}{3}}A_2^{\frac{1}{3}}(A_1^{\frac{1}{3}}+A_2^{\frac{1}{3}})$. The consequences of the model are discussed in detail. It is shown that a large body of data on fusion barriers and fusion cross sections can be reproduced. Predictions are made for heavier systems and higher energies than have been accessible so far.

1. Introduction

The presently available experimental evidence on compound nucleus formation, or "complete fusion", in heavy-ion collisions can be summarized qualitatively as follows:

(i) The fusion cross section (σ_{fu}) is usually smaller than the total reaction cross section (σ_{int}); the ratio σ_{fu}/σ_{int} decreases with increasing mass (charge) of either projectile or target at comparable incident energies per nucleon [1-4]).

(ii) The angular momentum limit for fusion (l_{fu}) usually increases with increasing bombarding energy, whereas the ratio σ_{fu}/σ_{int} is rather insensitive to energy [4-6]).

(iii) For a given compound system at a given excitation energy, l_{fu} depends on the initial fragmentation; it is therefore a property of the entrance channel, and not of the compound nucleus [7,8]).

In the following (sects. 2–7) we present classical calculations, which reproduce these features in considerable detail and make specific predictions for heavier systems and higher energies than have been accessible so far. A brief outline of the model used in these calculations has been published in a recent letter [9]).

Previous theoretical work on the fusion problem has mainly concentrated on two aspects: The effects of dynamic distortion on the Coulomb barrier [10-12]) and the stability of the compound nucleus against fission [13-15]). The decisive influence of entrance channel dynamics on the fusion cross section has been discussed by Swiatecki [ref. [16])], but attempts to formulate the problem quantitatively have only been made very recently [9,17,18]). A brief comparative discussion of relevant work is given in sect. 8.

2. Two-body potential

We assume that the fragments are initially spherical and are not appreciably deformed during their approach. The latter assumption is supported both by measurements and by dynamical calculations of interaction barriers [10-12]). A two-body potential is introduced to describe the interaction of the fragments as a function of their c.m. separation r.

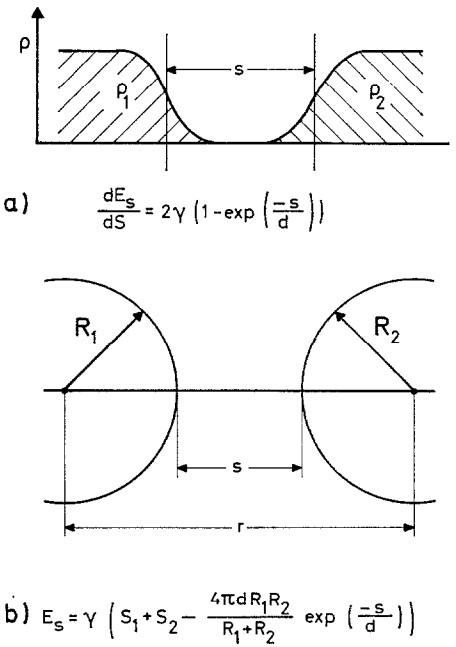

Fig. 1. Liquid drop model surface energy with finite range of interaction for two different geometries: (a) two plane, parallel surfaces; (b) two spherical nuclei.

The nuclear part of this interaction is derived from the liquid drop model, including effects of the finite range of nuclear forces in the following way: Let us consider nuclear matter in two semi-infinite regions, bounded by plane, parallel, diffuse surfaces at a distance s (measured between the planes of half-maximum density, see fig. 1). For the surface energy per unit area of this system we use the simple ansatz

$$\frac{dE_S}{dS} = 2\gamma \left\{1 - \exp\left(\frac{-s}{d}\right)\right\} \quad (s \geqq 0), \tag{1}$$

where γ is the specific surface energy of the liquid drop model. For two spheres with half-density radii R_1 and R_2 we obtain from eq. (1) by straight-forward geometrical arguments, neglecting terms of higher order in d/R_1 and d/R_2

$$E_S = \gamma \left\{S_1 + S_2 - \frac{4\pi d R_1 R_2}{R_1 + R_2} \exp\left(\frac{-s}{d}\right)\right\}. \tag{2}$$

The nuclear potential can now be identified with the difference in surface energies between finite and infinite separation s:

$$V_n = -4\pi\gamma \frac{dR_1R_2}{R_1+R_2} \exp\left(\frac{-s}{d}\right) \tag{3a}$$

$$= -a_S A_1^{\frac{1}{3}} A_2^{\frac{1}{3}} \frac{d}{R_{12}} \exp\left(-\frac{r-R_{12}}{d}\right). \tag{3b}$$

Here a_S is the surface term in the liquid drop model mass formula and $R_{12} = R_1+R_2 = r_0(A_1^{\frac{1}{3}}+A_2^{\frac{1}{3}})$ the sum of the half-maximum density radii. The nuclear potential for arbitrary fragment pairs and $r \geqq R_{12}$ is completely specified by eq. (2), except for the range parameter d, which is adjusted to fit experimental interaction barriers (see sect. 5).

The total effective potential between the fragments is composed of a Coulomb, nuclear and centrifugal part,

$$V_l(r) = \frac{Z_1Z_2e^2}{r} + \frac{\hbar^2l^2}{2\mu r^2} - a_S A_1^{\frac{1}{3}} A_2^{\frac{1}{3}} \frac{d}{R_{12}} \exp\left(-\frac{r-R_{12}}{d}\right). \tag{4}$$

The influence of fragment properties on this potential is conveniently expressed in terms of the dimensionless parameters

$$x = \frac{e^2}{r_0 a_S} \frac{Z_1Z_2}{A_1^{\frac{1}{3}}A_2^{\frac{1}{3}}(A_1^{\frac{1}{3}}+A_2^{\frac{1}{3}})}, \tag{5}$$

$$y = \frac{\hbar^2}{2m_0 r_0^2 a_S} \frac{A_1+A_2}{A_1^{\frac{4}{3}}A_2^{\frac{4}{3}}(A_1^{\frac{1}{3}}+A_2^{\frac{1}{3}})^2}, \tag{6}$$

where x is the ratio of the Coulomb force to the nuclear force and yl^2 the ratio of the centrifugal force to the nuclear force at the point of contact ($r = R_{12}$). These parameters have obvious counterparts in the liquid drop model theory of fission.

It should be stressed that the potential (4) is only defined in the external region ($r \geqq R_{12}$). In contrast to optical model potentials it is real by definition, since we use a classical description, in which intrinsic quantum states are not specified. In this picture, inelastic processes give rise to friction terms in the equations of motion, but do not eliminate the system from the quasi-elastic channel. The only absorptive mechanism is fusion, which occurs at $r = R_{12}$.

3. Friction

When the fragment density distributions start penetrating each other, energy will be dissipated in collisions between nucleons originating from different fragments. For the resulting friction force F we write

$$F_{12} = \int f(\rho_1, \rho_2)\{\langle v_1\rangle - \langle v_2\rangle\} dV \tag{7a}$$

$$\approx g(r)\{\langle v_1\rangle_{R_1} - \langle v_2\rangle_{R_2}\}, \tag{7b}$$

where $\langle v_i \rangle$ denotes a local average of nucleon velocities in fragment i and the subscript R_i refers to the half-maximum density point on the line connecting the fragment centres. The qualitative effects of this force are to slow down the radial fragment motion ("radial friction") and to transform relative angular momentum into intrinsic angular momentum of the fragments ("tangential friction"). Assuming that the intrinsic velocity fields of the fragments correspond to rigid rotation, we can derive the following coupled equations for their relative motion:

$$\mu \frac{\mathrm{d}^2 r}{\mathrm{d}t^2} + \frac{\mathrm{d}}{\mathrm{d}r} V_l(r) + g(r) \frac{\mathrm{d}r}{\mathrm{d}t} = 0, \tag{8}$$

$$\mu \frac{\mathrm{d}l}{\mathrm{d}t} + \tfrac{7}{2} g(r) \{ l - \tfrac{5}{7} l_\infty \} = 0. \tag{9}$$

Here l is the time-dependent angular momentum of relative motion, and l_∞ its asymptotic value before the collision.

In the calculations performed so far, we have made a further drastic simplification by considering only the limit of strong, sharply localized friction,

$$g(r) = g\delta(r - R_{12}) \qquad g \to \infty. \tag{10}$$

In this approximation, no loss of energy or orbital angular momentum occurs at $r > R_{12}$, and eqns. (8) and (9) are decoupled. When the point of contact is reached, the radial velocity drops sharply to zero, and the angular momentum from its asymptotic value l_∞ to $\frac{5}{7} l_\infty$.

In order to keep the formulation as general as possible, we replace in the following the numerical factor $\frac{5}{7}$ by the symbol f. Values of $f \neq \frac{5}{7}$ would then reflect deviations of the fragment moments of inertia from their rigid body values, or a more complicated coupling of the fragments than due to a strong tangential force acting at the contact point. It should be mentioned that the latter assumption, leading to $f = \frac{5}{7}$, implies for $A_1 \neq A_2$ opposite intrinsic rotation of the two fragments in a coordinate system rotating with the fragment centres. Rigid rotation of the two-fragment system as a whole, on the other hand, would in general require additional angular momentum transfer and result in

$$f = \left\{ 1 + \frac{2}{5} \left(\frac{m_1 R_1^2}{\mu R_{12}^2} + \frac{m_2 R_2^2}{\mu R_{12}^2} \right) \right\}^{-1}. \tag{11}$$

It is easily verified, that eq. (11) yields $f = \frac{5}{7}$ for $A_1 = A_2$ and $f < \frac{5}{7}$ for $A_1 \neq A_2$. In the calculations reported in this paper $f = \frac{5}{7}$ has been used.

There are several arguments, why this obviously crude model might be a useful starting point: Firstly its mathematical simplicity enables one to explore its consequences for arbitrary fragment pairs without computational effort. Secondly, it seems intuitively plausible, that the friction force increases sharply, when the density in the overlap region approaches saturation density of nuclear matter. The reason is

that with increasing local fragment densities nucleon-nucleon collisions not only become more frequent, but also have to occur with larger momentum transfers due to the Pauli principle. Finally, a comparison of calculated fusion barriers with experimental data indicates that energy losses, at distances where only the tails of the density distributions overlap, are relatively small (see sect. 5).

4. Energy dependence of the fusion cross section

The consequences of the model developed so far are shown schematically in fig. 2 for a fragment pair with $x < 1$. Plotted is the limiting value of $l^2 (= \sigma/\pi\lambda^2)$ for different processes as a function of bombarding energy $E_{c.m.}$. The highest limit corresponds to the total reaction cross section, which has been calculated with an energy-independent interaction radius (see sect. 5).

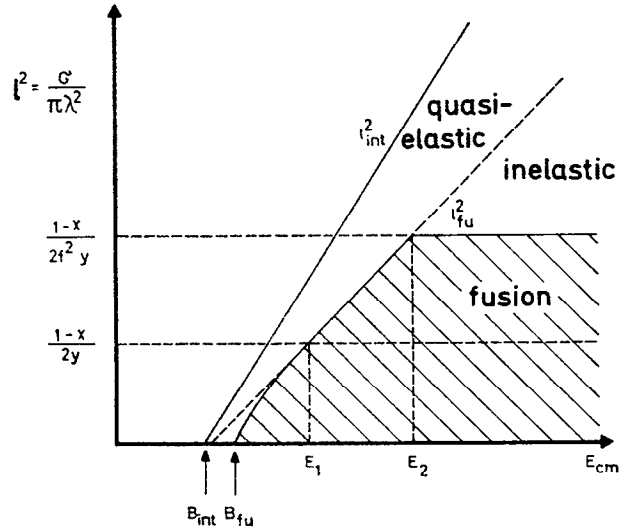

Fig. 2. Angular momentum limits for different processes as functions of bombarding energy. For definition of the symbols see text.

In discussing the limiting angular momentum for fusion, we have to distinguish three different energy regions. At bombarding energies below

$$E_1 = \frac{Z_1 Z_2 e^2}{R_{12}} \left\{ 1 + \frac{1-x}{2x} - \frac{1}{x} \frac{d}{R_{12}} \right\}, \tag{12}$$

the limit l_{fu} is determined by the condition that the energy of relative motion must be equal to the maximum of the corresponding potential V_l (eq. (4)). The distance r, at which this maximum occurs, decreases with increasing values of l_{fu} and $E_{c.m.}$, and coincides with R_{12} for $E_{c.m.} = E_1$. The angular momentum limit for fusion at E_1 is

$$l_{fu}(E_1) = \left\{ \frac{1-x}{2y} \right\}^{\frac{1}{2}}. \tag{13}$$

For $E_{c.m.} > E_1$ the fragments penetrate to R_{12}, where – according to the assumptions outlined in sect. 3 – friction effects come into play. These result in a complete stop of the radial motion and a reduction of the orbital angular momentum by the factor $1/f$ ($f < 1$). We assume at this point that the contact configuration will either fuse or separate, depending on whether the resultant of the Coulomb, centrifugal and nuclear forces is attractive or repulsive (see, however, sect. 7). This condition defines a critical post-friction angular momentum, at which the repulsive Coulomb and centrifugal forces are just counterbalanced by the attractive nuclear force; its value is given by eq. (13).

At energies $E_{c.m.}$ between E_1 and

$$E_2 = \frac{Z_1 Z_2 e^2}{R_{12}} \left\{ 1 + \frac{1}{f^2} \frac{1-x}{2x} - \frac{1}{x} \frac{d}{R_{12}} \right\}, \tag{14}$$

the angular momentum at R_{12} is reduced sufficiently by tangential friction to remain below the critical post-friction value. In this energy region fusion occurs for all fragment pairs, which penetrate to R_{12}.

At still higher energies, $E_{c.m.} > E_2$, the maximum post-friction angular momentum at R_{12} exceeds the critical value (eq. (13)); consequently, the asymptotic (pre-friction) angular momentum saturates at the value

$$l_{fu}(E_2) = \frac{1}{f} \left\{ \frac{1-x}{2y} \right\}^{\frac{1}{2}}, \tag{15}$$

where the factor f, as before, denotes the change in relative angular momentum due to tangential friction; it may be recalled that the assumptions discussed in sect. 3 yield $f = \frac{5}{7}$.

It is important to note that fusion is excluded in the present model for systems with $x > 1$, or

$$\frac{Z_1 Z_2}{A_1^{\frac{1}{3}} A_2^{\frac{1}{3}} (A_1^{\frac{1}{3}} + A_2^{\frac{1}{3}})} > \frac{r_0 a_S}{e^2}. \tag{16}$$

In the present calculations we have used $r_0 = 1.07$ fm and $a_S = 17.0$ MeV (without symmetry correction), resulting in the value 12.6 for the right hand side of eq. (16).

We close this section by summarizing the main results: The energy dependence of the fusion cross section is governed at low energies ($< E_1$) by properties of the two-body potential, and at higher energies by friction effects. Radial friction is assumed to completely dissipate the radial kinetic energy at R_{12}; this leads to saturation of the limiting angular momentum l_{fu} at higher energies ($> E_2$) and prevents fusion of systems with $x > 1$. Tangential friction, on the other hand, stabilizes the contact configuration by reducing the centrifugal force; as a result, the saturation value of the limiting angular momentum is increased from $l_{fu}(E_1)$ to $l_{fu}(E_2)$ by a factor $1/f$ ($= \frac{7}{5}$).

5. Interaction barriers and fusion barriers

It is important to realize that the "Colulomb barriers" for quasi-elastic surface reactions and for fusion are in general different. This distinction has not been widely recognized in the literature so far. The physical background is very simple: The quasi-elastic processes – resulting in relatively small mass and (or) energy transfer – become significant as soon as the fragments approach to within the range of nuclear forces. At this point, however, the resultant of the Coulomb and nuclear forces is still repulsive for sufficiently heavy systems, and additional energy is required to get the fragments over their mutual potential barrier.

In the following we define as "interaction barrier" B_{int} the threshold for (quasi-elastic) nuclear reactions. Theoretically we identify B_{int} with that bombarding energy, for which the distance of closest approach in a head-on collision becomes equal to or less than $R_{12}+d_{\mathrm{int}}$, where the "interaction distance" d_{int} is assumed equal for all fragment pairs and adjusted to fit experimental interaction barriers.

The fusion barrier B_{fu}, on the other hand, is equal to the height of the potential barrier for zero angular momentum, which is located at $r = R_{12}+d_{\mathrm{fu}}$. In contrast to d_{int}, the "fusion distance" d_{fu} depends on the fragment pair according to the following approximate relationship (from eqs. (4), (5))

$$\frac{d_{\mathrm{fu}}}{d} \approx -\ln x \left(1-2\frac{d}{R_{12}}\right)^{-1}. \tag{17}$$

The barriers B_{fu} and B_{int} are now given by

$$B_{\mathrm{fu}} = \frac{Z_1 Z_2 e^2}{R_{12}}\left\{\frac{R_{12}}{R_{12}+d_{\mathrm{fu}}} - \frac{1}{x}\frac{d}{R_{12}}\exp\left(\frac{-d_{\mathrm{fu}}}{d}\right)\right\}, \tag{18}$$

$$B_{\mathrm{int}} = \frac{Z_1 Z_2 e^2}{R_{12}}\left\{\frac{R_{12}}{R_{12}+d_{\mathrm{int}}} - \frac{1}{x}\frac{d}{R_{12}}\exp\left(\frac{-d_{\mathrm{int}}}{d}\right)\right\} \quad (d_{\mathrm{fu}} < d_{\mathrm{int}}) \tag{19a}$$

$$= B_{\mathrm{fu}} \quad (d_{\mathrm{fu}} > d_{\mathrm{int}}). \tag{19b}$$

These expressions contain two adjustable parameters: The range d of the nuclear interaction and the interaction distance d_{int}.

For comparatively light projectiles ($A \approx 12$–16) the interaction barrier B_{int} depends mainly on d, but very little on d_{int}, whereas the opposite holds for heavier projectiles (^{40}Ar, ^{84}Kr) and heavy targets. Therefore both parameters can be determined from a fit of eq. (19) to experimental interaction barriers over a wide range of target and projectile masses. The result is $d = 1.35$ fm and $d_{\mathrm{int}} = 2d = 2.70$ fm. These values are based on $R_{12} = r_0(A_1^{\frac{1}{3}}+A_2^{\frac{1}{3}})$ with $r_0 = 1.07$ fm; other choices of r_0 will result in slightly different values of d and d_{int}. Inserting the above numbers, eq. (19a) can be re-written as

$$B_{\mathrm{int}} = \frac{Z_1 Z_2 e^2}{R_{12}+2.70\,\mathrm{fm}} - 2.90\ \mathrm{MeV}\,\frac{A_1^{\frac{1}{3}}A_2^{\frac{1}{3}}}{A_1^{\frac{1}{3}}+A_2^{\frac{1}{3}}}. \tag{20}$$

The fusion barriers B_{fu} are now determined by eqs. (17) and (18) without further parameter adjustment.

A comparison of calculated and experimental barriers is given in table 1. The uncertainties of the experimental values are difficult to assess, especially since some of the values given in table 1 represent the present authors interpretation of published data. It appears, however, that the calculation reproduces practically all of the results within experimental accuracy, and that interaction barriers can be predicted to within $\pm 2\,\%$ for projectiles up to Kr. Unfortunately, only few fusion barriers have been measured; the available evidence seems consistent with the present calculation and clearly supports the prediction of a difference $(B_{fu} - B_{int})$, which increases with increasing target and projectile mass and reaches about 30 MeV for Kr on heavy targets. Calculated and measured barriers for ^{84}Kr projectiles as functions of target atomic number are shown in fig. 3.

Two points deserve further comment: Firstly, there is no evidence for a systematic lowering of the barriers due to static deformation of either target or projectile. The present analysis suggests, that this effect is considerably smaller than its predicted size of about 8 % [ref. [28])]. Secondly, it should be stressed, that within the present model the difference $(B_{fu} - B_{int})$ is a property of the quasi-elastic two-body potential, and not due to energy loss by friction. Strong friction at distances $r > R_{12}$ would increase this difference, especially for systems where $d_{fu} \ll d_{int}$ (see table 1). The observed correspondence between calculated and measured barriers may be taken as evidence in favour of the present potential and the assumed absence of significant friction at large distances.

TABLE 1

Interaction barriers (B_{int}) and fusion barriers (B_{fu}) (all energies in the c.m. system)

Projectile	Target	Calculated values			Experimental values		
		B_{int} (MeV)	B_{fu} (MeV)	d_{fu} (fm)	B_{int} (MeV)	B_{fu} (MeV)	Ref.
^{12}C	^{205}Tl	56.2	57.0	2.09	56		[19])
	^{209}Bi	57.5	58.3	2.02	57		[19])
	^{238}U	62.7	63.7	1.94	62.2		[20])
^{14}N	^{238}U	72.7	74.2	1.75	73.4		[20])
^{16}O	^{205}Tl	74.5	76.1	1.75	77		[19])
	^{238}U	82.6	85.3	1.62	82.5		[20])
^{20}Ne	^{238}U	103	107	1.35	102		[20])
^{32}S	^{40}Ca	42.5	42.8	2.28		43.5	[21])
	^{58}Ni	58.0	59.2	1.88		59.5	[21])
^{40}Ar	^{121}Sb	106	111	1.28		111	[4])
	^{164}Dy	134	141	1.09	135		[22])
	^{238}U	177	190	0.80	171		[23])
^{74}Ge	^{232}Th	294	322	0.28	290	310	[24])
^{84}Kr	^{72}Ge	134	142	1.02		147	[25])
	^{116}Cd	190	206	0.68		204	[25])
	^{209}Bi	306	336	0.22		(< 357)	[26])
	^{232}Th	326	359	0.17	332		[27])
	^{238}U	332	367	0.15	333	(> 370)	[26])

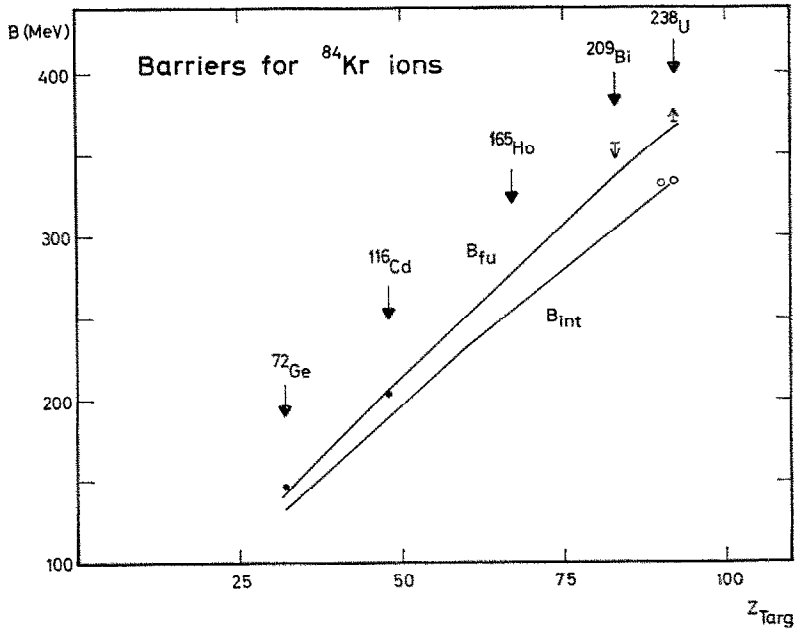

Fig. 3. Comparison of calculated and measured fusion barriers (B_{fu}) and interaction barriers (B_{int}) for ^{84}Kr projectiles incident on different target nuclei (solid points and arrows: experimental fusion barriers or limits; open circles: experimental interaction barriers; for numerical values and references see table 1).

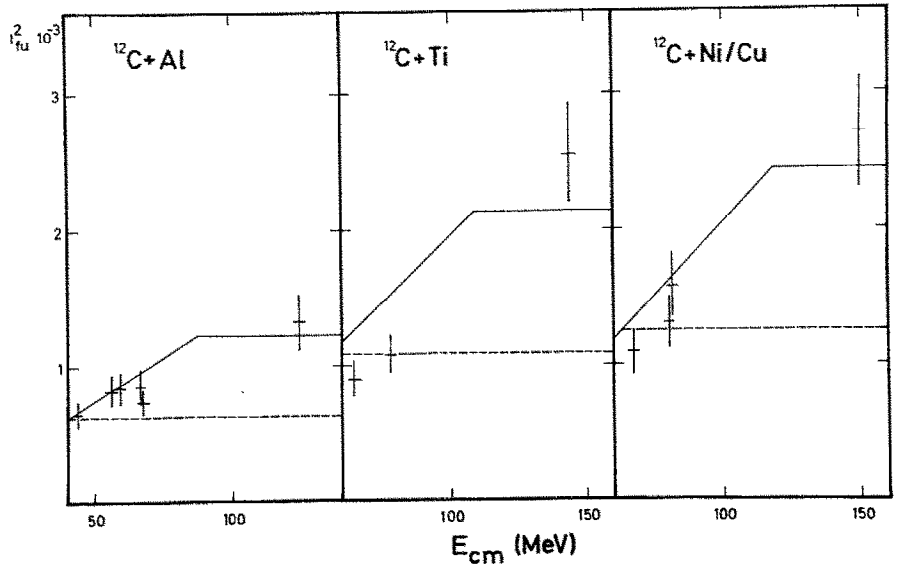

Fig. 4. Comparison of calculated and measured angular momentum limits for fusion of ^{12}C projectiles with different target nuclei (experimental data from ref. [6]).

6. Comparison of calculated and measured fusion cross sections

In figs. 4–7 we compare calculated fusion cross sections with published experimental data. As in fig. 2, a representation of $l^2 = \sigma/\pi\lambda^2$ versus c.m. bombarding energy has been chosen; in comparing with cross-section excitation functions it must be kept in mind, that σ is proportional to $l^2 E_{\mathrm{c.m.}}^{-1}$.

In selecting the material for figs. 4–7 our main concern has been to exhibit the dependence of the fusion cross section on either energy, projectile mass or target mass, rather than to present a comparison for as many isolated data points as possible. Some preference has been given to results for heavier projectiles and (or) targets, as the present model should be most appropriate for rather heavy nuclei. Except for the data shown in fig. 4, the fission channel has been included in the complete fusion cross section.

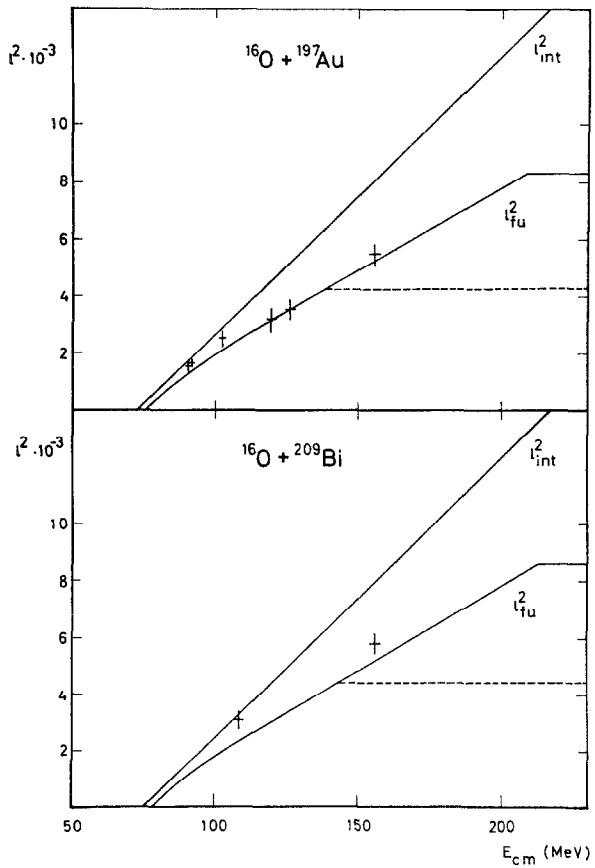

Fig. 5. Comparison of calculated and measured angular momentum limits for fusion of ^{16}O projectiles with ^{197}Au and ^{209}Bi targets (experimental data from refs. [2, 29]).

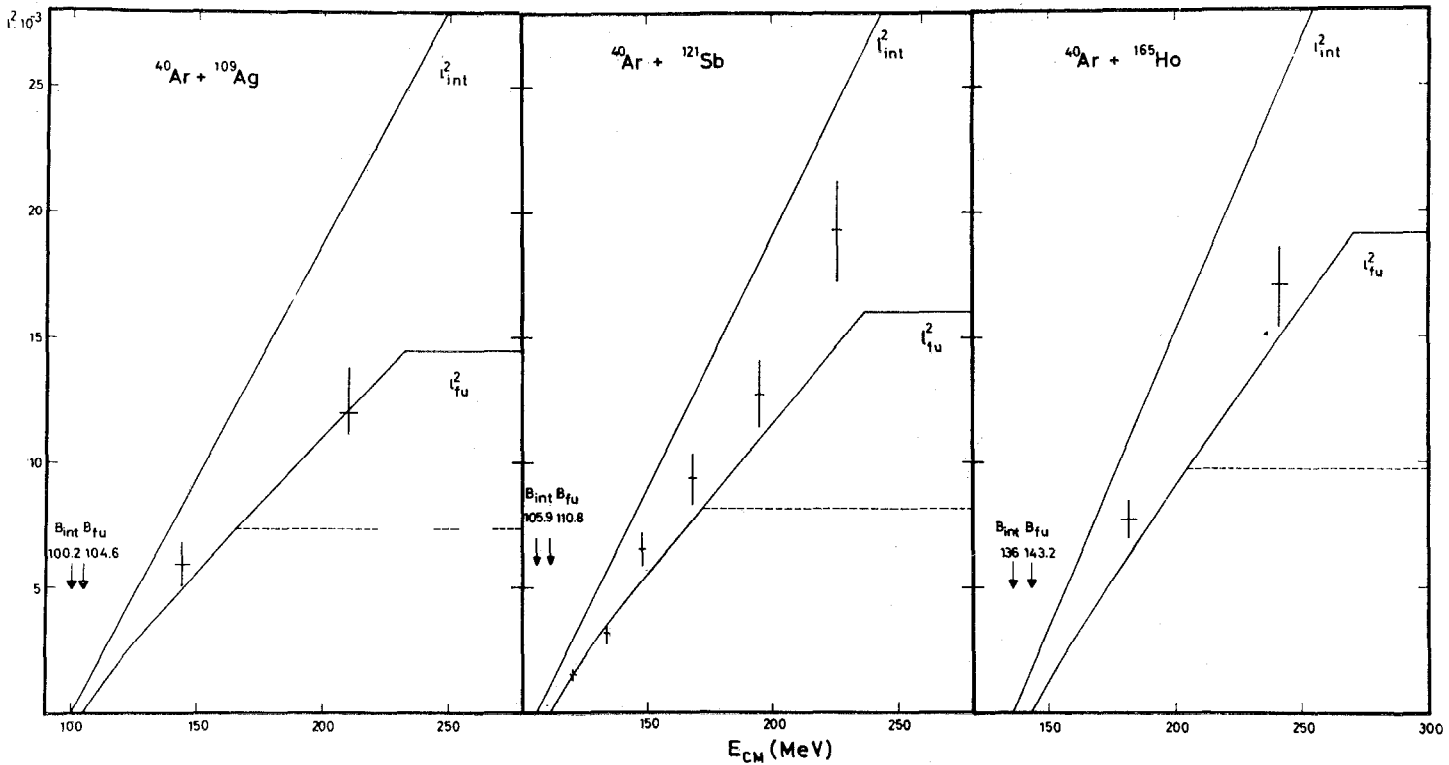

Fig. 6. Comparison of calculated and measured angular momentum limits for fusion of ^{40}Ar projectiles with different target nuclei (experimental data from refs. [4, 5]).

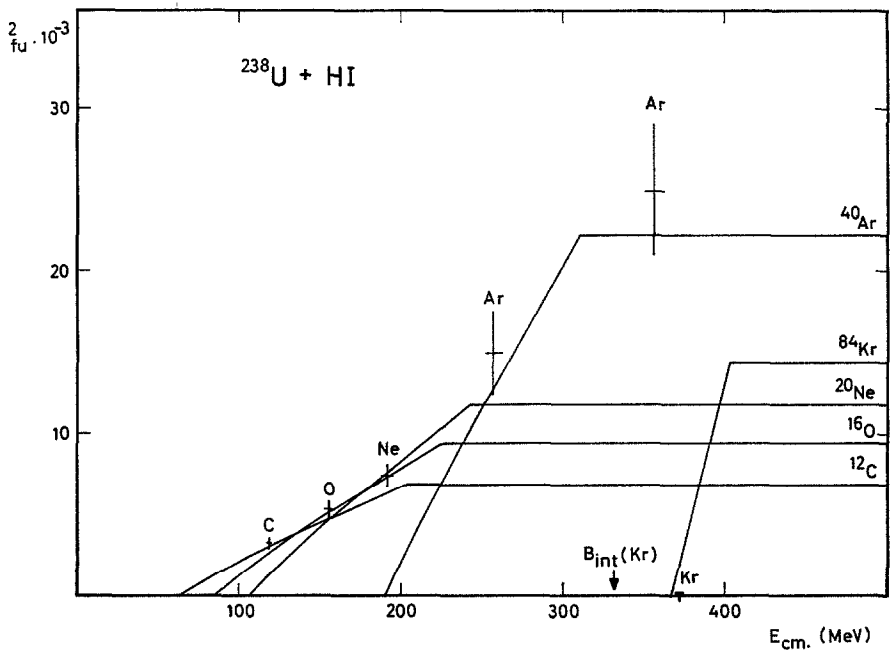

Fig. 7. Comparison of calculated and measured angular momentum limits for fusion of different projectiles with ^{238}U target nuclei (experimental data from refs. [3,26]).

The overall agreement between calculated and measured fusion cross sections, as shown in figs. 4–7, is quite remarkable considering the simplicity of the present model. This strongly supports our assumption that the transition to fusion occurs near the point where the fragment densities in the overlap region add up to saturation density of nuclear matter. The broken horizontal lines in figs. 4–6 show, where l_{fu}^2 would saturate in the absence of angular momentum transfer by tangential friction, but with strong radial friction at $r = R_{12}$. The fact, that l_{fu}^2 continues to increase with energy beyond that level suggests that tangential friction is indeed important. Unfortunately, the bulk of available data does not extend to high enough energies to provide a significant test on the predicted saturation of l_{fu}^2 at $E_{c.m.} \geqq E_2$ (eq. (14)). Thus detailed conclusions concerning friction effects must await further experimental evidence for higher bombarding energies or heavier systems.

7. Fission via fragment deformation

In this section we discuss the evolution of the two-fragment system after contact has been established and the radial motion has been slowed down. So far it has been assumed that the contact configuration will collapse into a compound nucleus, whenever the radial force between the fragments is attractive. In order to examine this assumption more closely, we consider a situation where appreciable penetration

of the fragments is still excluded, but the fragment surfaces are allowed to undergo axially symmetric quadrupole deformations with amplitudes β_1 and β_2. In this picture, oblate deformation of both fragments (β_1, $\beta_2 < 0$) corresponds to the build-up of a neck, which leads to an increase in the cohesive nuclear force (counteracted, however, by stronger Coulomb repulsion) and eventually to fusion of the fragments. Prolate deformation (β_1, $\beta_2 > 0$), on the other hand, has the opposite effect and results in fission.

In order to obtain quantitative estimates, we write for the effective potential of the fragment-fragment system

$$V_l(s, \beta_1, \beta_2) = V_1(\beta_1) + V_2(\beta_2) + V_C(1,2) + V_n(1,2) + \frac{l^2\hbar^2}{2\mu r^2}, \tag{21}$$

where $V_1(\beta_1)$ and $V_2(\beta_2)$ refer to the isolated fragments and depend quadratically on β for small deformations, and r, as before, is the separation of the fragment centres of mass. The variable s denotes the distance between the points of half-maximum density (see fig. 2) and is given by

$$s = r - R_{12} - R_1\beta_1 - R_2\beta_2. \tag{22}$$

The Coulomb interaction $V_C(1,2)$ has been taken from ref. [11]) and the nuclear interaction $V_n(1,2)$ is derived from eq. (3) (where R_1, R_2 have to be interpreted as the radii of curvature at the point of contact). Neglecting higher-order terms in β_1, β_2 we obtain

$$V_C(1,2) = \frac{Z_1 Z_2 e^2}{r}\left\{1 + \frac{3}{5}\left(\frac{R_1^2}{r^2}\beta_1 + \frac{R_2^2}{r^2}\beta_2\right) + \ldots\right\}, \tag{23}$$

$$V_n(1,2) = -a_S A_1^{\frac{1}{3}} A_2^{\frac{1}{3}} \frac{d}{R_{12}} \exp\left(\frac{-s}{d}\right)\left\{1 - 4\left(\frac{R_2}{R_{12}}\beta_1 + \frac{R_1}{R_{12}}\beta_2\right) + \ldots\right\}. \tag{24}$$

We assume that the fragments are initially ($t = 0$) touching and spherical (s, β_1, $\beta_2 = 0$) and held together by an attractive force ($(\partial V_l/\partial s) > 0$). For $t > 0$, the fragments will remain in contact, but start to deform. We further assume that the system follows the line of steepest descent of $V_l(0, \beta_1, \beta_2)$ in the β_1, β_2 plane, and that it will undergo fusion (fission), if this corresponds to an increase (decrease) in radial attraction ($\partial V_l/\partial s$). With these assumptions, fusion will occur if the inequality

$$\left\{\frac{\partial V_l}{\partial \beta_1}\frac{\partial^2 V_l}{\partial s \partial \beta_1} + \frac{\partial V_l}{\partial \beta_2}\frac{\partial^2 V_l}{\partial s \partial \beta_2}\right\}_{s, \beta_1, \beta_2 = 0} < 0 \tag{25}$$

is satisfied, but not otherwise.

Calculations have been performed to investigate the consequences of condition (25) for different fragment pairs. The results are conveniently expressed in terms of the parameter x (eq. (5)) and a radius asymmetry parameter $|R_2 - R_1|/(R_2 + R_1)$. They indicate that the fusion cross section should be severely limited compared to pre-

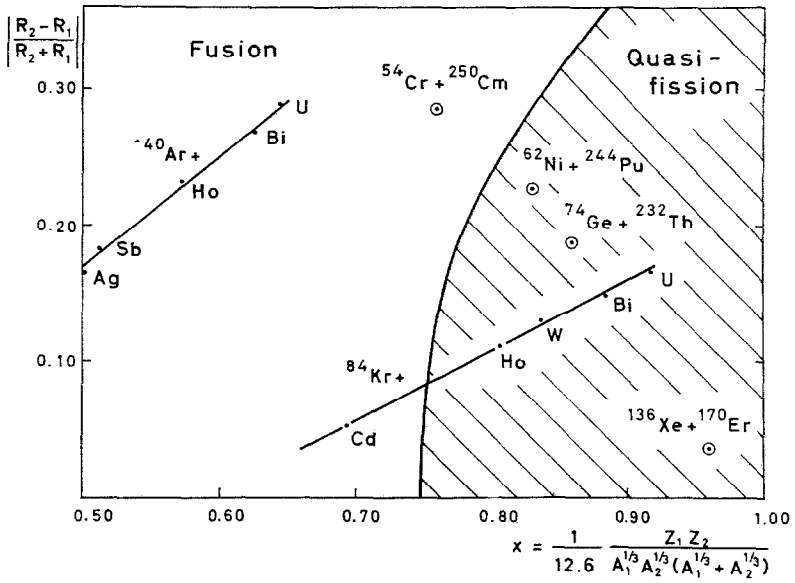

Fig. 8. Calculated regions of fusion and quasi-fission of a contact configuration of two originally spherical fragments at zero relative angular momentum. The straight lines connect systems produced by either ^{40}Ar or ^{84}Kr bombardment of different target nuclei; the concentric points and circles are systems of interest for the production of superheavy nuclei.

dictions of the deformation-independent model, for systems with x approaching unity and moderate asymmetry. Fig. 8 shows the predicted region in the asymmetry-versus-x plane, where fusion should be completely forbidden due to instability of the contact configuration against fission at zero angular momentum. According to these calculations, complete fusion should not be observable in the krypton bombardment of heavy target nuclei and with the more symmetric fragment pairs of interest for superheavy production.

Fig. 9 shows calculated angular momentum limits for the interaction of ^{40}Ar and ^{84}Kr projectiles with different target nuclei. The upper curve in each diagram is the limit for initial radial stability of the contact configuration, as calculated in the deformation-independent model. The lower curves are limits for complete fusion, taking deformation into account. Between the curves, the contact configuration should decay by fission via fragment deformation ("quasi-fission").

Obviously, these simple-minded calculations cannot be expected to yield quantitatively accurate results. They are, however, qualitatively consistent with existing experimental evidence on krypton-induced reactions with heavy targets [4,26]. In these studies significant yields have been observed of highly inelastic events in which products with masses close to those of the original fragments were emitted. Yields of products corresponding to nearly symmetric fission of a compound nucleus were comparatively small or absent in krypton bombardments, but dominated in argon

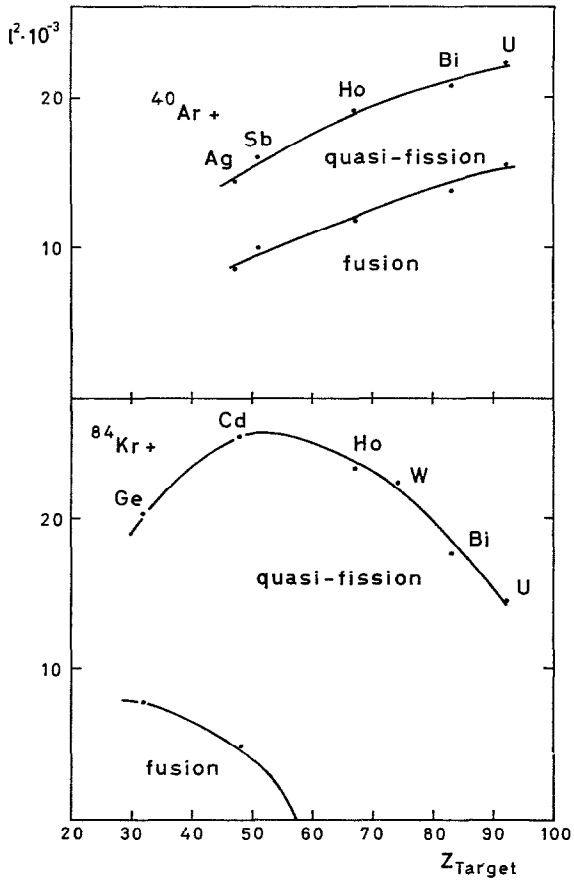

Fig. 9. Calculated angular momentum limits for fusion and quasi-fission of systems produced by either ^{40}Ar or ^{84}Kr bombardment of different target nuclei.

bombardments of comparable targets. These general features are well reproduced in the present calculations.

The results shown in fig. 9 suggest appreciable admixtures of the quasi-fission mode also in the case of ^{40}Ar induced fusion at higher bombarding energies. These events should be similar to compound nucleus fission with respect to fragment energies and angular distributions, but yield mass distributions sharply peaked near the projectile and target mass. Whether or not such events were present in existing measurements (see figs. 6, 7) and included in the quoted fission cross sections, is difficult to judge. The observed agreement with the deformation-independent model (sect. 6) indicates that the present approach somewhat overestimates the quasi-fission component, unless it has been included in significant measure in some of the experimental fusion cross sections shown in figs. 6 and 7. Clearly more detailed experimental studies would be of interest.

To conclude this section, we briefly comment on the consequences of fig. 8 for the production of superheavy nuclei by fusion reactions. The results clearly suggest that compound nucleus formation is most likely to be achieved for the most asymmetric target-projectile combinations. A similar conclusion has been reached several years ago by Swiatecki [16]). The problem is that compound nuclei resulting from very asymmetric fragmentations at the fusion barrier are expected to have significantly higher excitation energies – and thus a smaller chance of survival against fission – than those resulting from more symmetric fragmentations [9]). The success of superheavy production therefore depends on whether target-projectile combinations can be found which represent a suitable balance between the conflicting requirements of compound nucleus formation and compound nucleus survival.

8. Conclusions and outlook

The present calculations show that many of the observed properties of fusion reactions can be understood in terms of classical potential scattering. The transition from the entrance channel to the compound nucleus seems to occur at a well defined distance, where the fragment densities in the overlap region add up to saturation density of nuclear matter. This feature has been reproduced in the calculations by assuming that friction effects – leading to dissipation of energy and angular momentum – set in strongly at the point of contact. A further consequence of this assumption is the prediction that the limiting angular momentum for fusion should saturate at higher energies, and that fusion should be forbidden for systems with $x > 1$.

The results summarized above depend in large measure on the choice of a suitable two-body potential. This has been deduced here from the liquid drop model by inclusion of a finite range of interaction, as proposed originally by Scheid *et al.* [30]). Similar potentials have been suggested recently by Krappe and Nix [31]) and by Wilczynski [17]). The present ansatz is not basically different from the results of these authors, but has the advantage of greater mathematical simplicity which leads to a very convenient formulation of the fusion problem in terms of dimensionless parameters.

An alternative approach to the problem of the quasi-elastic nucleus-nucleus potential has been followed by Brink and Rowley [32]) and by Gross and Kalinowski [ref. [18])]. These authors construct a two-body potential by folding the real part of the target-nucleon optical model potential with the nucleonic density distribution of the projectile. Several objections may be raised against the use of such a potential in the present context: Firstly the relevance of the optical model, which implies projection of a definite quantum state, to a classical calculation like the present one is not obvious; secondly many-body effects are neglected, which should be implicit in the liquid drop model. A rather obvious defect of the folding prescription, its lack of invariance under exchange of target and projectile, may be repaired formally by symmetrization [18]).

Limiting angular momenta for fusion have been calculated by Wilczynski [17]) and by Gross and Kalinowski [18]). In the former work, friction effects are not explicitly discussed; fusion is assumed to occur when the effective fragment-fragment interaction in the contact configuration, as calculated with the asymptotic angular momentum, is attractive. The results are in fair agreement with a large number of measurements, but do not reproduce the large fusion cross sections observed with ^{40}Ar projectiles at higher bombarding energies [5]). According to the present analysis this discrepancy results from the neglect of angular momentum transfer by tangential friction.

Gross and Kalinowski [18]) have performed numerical calculations of the nucleus-nucleus scattering problem including friction. Their friction tensor is highly anisotropic, with dominant radial friction but independent of fragment masses and energy. It has a Saxon-Woods radial form factor with a radius corresponding to the interaction radius of the present work ($R_{12}+2.70$ fm, see sect. 5). In contrast to the present assumptions, this model predicts large energy losses of the order of 50 MeV, at distances well outside the point of contact ($r = R_{12}$). Capture into the compound nucleus also must occur at significantly larger distances, since the authors state that all of their scattering trajectories keep outside 1.2 $(A_1^{\frac{1}{3}}+A_2^{\frac{1}{3}})$ fm. The calculated angular momentum limits for fusion are in excellent agreement with existing data, except for krypton bombardments, where large fusion cross sections are predicted in contrast to observation.

The comparison of ref. [18]) with the present work shows that very different assumptions can produce very similar fusion cross sections. In the case at hand, this seems to arise from an approximate cancellation of two dominant effects: The use, in ref. [18]), of the more attractive folding potential shifts the barrier for the critical partial wave towards larger radii and smaller energies. This difference in barrier height, however, is dissipated by radial friction while the fragments approach the barrier.

Ambiguities of this kind can only be resolved by additional measurements and more comprehensive analyses, including barrier information and – where available – quasielastic scattering data. In the following we comment briefly on possible improvements of the present model.

A better description of individual fragment pairs could undoubtedly be achieved by suitable adjustments of the parameters a_S, r_0 and d. However, in order to retain the simplicity of the present approach – in the spirit of the liquid drop model – it seems preferable to use universal values, readjusting them, if necessary, by a global fit to fusion and scattering data. Most important, in this context, will be data for systems with $x \approx 1$.

The validity of the present schematic treatment of friction should be investigated by more realistic calculations, based on eqs. (7)–(9). Fink and Toepffer have recently developed a dynamical absorption model for scattering which applies phase space arguments to nucleon-nucleon collisions in the region of overlap [33]). This model seems to be a very promising starting point for a parameter-free microscopic derivation of eq. (7).

For high bombarding energies and comparatively light projectiles the present assumption of complete slowing down at $r = R_{12}$ by radial friction will probably be unrealistic and some penetration of the fragments must be expected. Under these circumstances the tangential coupling between the fragments will be more rigid than that due to a contact force, and a transition from $f = \frac{5}{7}$ to f given by eq. (11) will occur. Consequently, the angular momentum limit for fusion of asymmetric fragment pairs may significantly exceed the saturation value expected for $f = \frac{5}{7}$ (see eq. (15)). Possible evidence for such an effect comes from recent measurements by Namboodiri *et al.* with 262 MeV ^{14}N projectiles on Al, Cr and Ni targets [34]).

Instructive discussions and correspondence with W. Greiner, J. Huizenga, J. B. Natowitz, W. Scheid and C. Toepffer are gratefully acknowledged.

References

1) L. Kowalski, J. C. Jodogne and J. M. Miller, Phys. Rev. **169** (1968) 894
2) J. B. Natowitz, Phys. Rev. **C1** (1970) 623
3) T. Sikkeland and V. E. Viola, Proc. Third Conf. on reactions between complex nuclei, Asilomar 1963, ed. A. Ghiorso, R. M. Diamond and H. E. Conzett (Univ. of California Press, 1963) p. 232; T. Sikkeland, Phys. Lett. **27B** (1968) 277
4) M. Lefort *et al.*, Orsay report IPNO-RC-73-04 (1973)
5) H. H. Gutbrod *et al.*, IAEA-SM-174/59, presented at Third Symp. on the physics and chemistry of fission, Rochester NY 1973
6) J. B. Natowitz, E. T. Chulik and M. N. Namboodiri, Phys. Rev. **C6** (1972) 2133
7) A. M. Zebelman and J. M. Miller, Phys. Rev. Lett. **30** (1973) 27
8) J. Galin *et al.*, Orsay reports IPNO-RC-73-03 (1973) and IPNO-RC-73-07 (1973)
9) R. Bass, Phys. Lett. **47B** (1973) 139
10) H. Holm, W. Scheid and W. Greiner, Phys. Lett. **29B** (1969) 473; H. Holm and W. Greiner, Phys. Rev. Lett. **24** (1970) 404; Nucl. Phys. **A195** (1972) 333
11) P. W. Riesenfeldt and T. D. Thomas, Phys. Rev. **C2** (1970) 2448
12) A. S. Jensen and C. Y. Wong, Phys. Lett. **32B** (1970) 567; Nucl. Phys. **A171** (1971) 1
13) B. N. Kalinkin and I. Z. Petkov, Acta Phys. Pol. **25** (1964) 265
14) S. Cohen, F. Plasil and W. J. Swiatecki, Proc. Third Conf. on reactions between complex nuclei, Asilomar 1963, ed. A. Ghiorso, R. M. Diamond and H. E. Conzett (Univ. of California Press, 1963) p. 325
15) M. Blann and F. Plasil, Phys. Rev. Lett. **29** (1972) 303
16) W. J. Swiatecki, in Nuclear reactions with heavy ions, Proc. Int. Conf., Heidelberg 1969, ed. R. Bock and W. R. Hering (North-Holland, Amsterdam, 1970) p. 729
17) J. Wilczynski, Nucl. Phys. **A216** (1973) 386
18) D. H. E. Gross and H. Kalinowski, Phys. Lett. **48B** (1974) 302
19) Y. Le Beyec, M. Lefort and M. Sarda, Nucl. Phys. **A192** (1972) 405
20) V. E. Viola, Jr. and T. Sikkeland, Phys. Rev. **128** (1962) 767
21) H. H. Gutbrod, W. G. Winn and M. Blann, Phys. Rev. Lett. **30** (1972) 1259
22) Y. Le Beyec, M. Lefort and A. Vigny, Phys. Rev. **C3** (1971) 1268
23) T. Sikkeland, Ark. Fys. **36** (1966) 539
24) Y. T. Oganessian, Proc. Int. Conf. on nuclear physics, Munich 1973, vol. 2, ed. J. de Boer and H. J. Mang (North-Holland, Amsterdam, 1973) p. 352
25) H. Gauvin *et al.*, Phys. Rev. Lett. **28** (1972) 697
26) M. Lefort *et al.*, Nucl. Phys. **A216** (1973) 166
27) R. Bimbot *et al.*, Nucl. Phys. **A189** (1972) 539
28) C. Y. Wong, Phys. Lett. **42B** (1972) 186

29) T. Sikkeland, Phys. Rev. **135** (1964) B669
30) W. Scheid, R. Ligensa and W. Greiner, Phys. Rev. Lett. **21** (1968) 1479;
W. Scheid and W. Greiner, Z. Phys. **226** (1969) 364
31) H. J. Krappe and J. R. Nix, IAEA-SM-174/12, presented at Third Symp. on the physics and chemistry of fission, Rochester NY 1973
32) D. M. Brink and N. Rowley, Nucl. Phys. **A219** (1974) 79
33) B. Fink and C. Toepffer, Phys. Lett. **45B** (1973) 411
34) J. B. Natowitz, private communication, 1974